Comparison of the Electrical Properties and Chemical Stability of Crystalline Silicon(111) Surfaces Alkylated Using Grignard Reagents or Olefins with Lewis Acid Catalysts

Lauren J. Webb and Nathan S. Lewis*

Division of Chemistry and Chemical Engineering, 210 Noyes Laboratory, 127-72, California Institute of Technology, Pasadena, California 91125

Received: October 22, 2002

Four methods were used to functionalize crystalline Si(111) surfaces with alkyl groups (C_nH_{2n+1}, $n = 1$, 2, 6, 8): chlorination with PCl_5 followed by alkylation with $C_nH_{2n+1}MgX$ (X = Cl, Br), chlorination with Cl_2(g) followed by alkylation with $C_nH_{2n+1}MgX$, Lewis acid-mediated reduction of a terminal alkene, and anodization in diethyl ether containing 3.0 M CH_3MgI. The chemical properties of each surface were characterized as a function of time exposed to air using X-ray photoelectron spectroscopy, and the electrical properties of the various surfaces were probed using time-resolved radio frequency (rf) photoconductivity decay methods. Both chlorination/alkylation routes produced alkylated Si surfaces that displayed low (<200 cm s^{-1}) initial charge carrier surface recombination velocities (*S*); furthermore, the recombination velocities of these functionalized surfaces were stable during >600 h of exposure to air. Surfaces functionalized through this route also displayed a significantly lower rate of oxidation than did unalkylated, H-terminated or Cl-terminated Si(111) surfaces. In contrast, surfaces modified by the Lewis acid-catalyzed reduction of 1-hexene and 1-octene exhibited high *S* values ($S > 400$ cm s^{-1}) when initially exposed to air and oxidized as rapidly as H-terminated Si(111) surfaces. Methyl-terminated Si(111) surfaces functionalized by anodization in a solution of CH_3MgI in ether exhibited stable, albeit high, *S* values (460 cm s^{-1}), indicating that the surface had been partially modified by the anodization process. The fractional monolayer coverage of oxide on the alkylated surface after exposure to air was determined for each functionalization technique. Although all four of the functionalization routes studied in this work introduced alkyl groups onto the Si surface, subtle changes in the extent and quality of the alkyl termination are significant factors in determining the magnitude and degree of chemical and electrical passivation of the resulting functionalized Si surfaces.

I. Introduction

Freshly prepared H-terminated Si(111) surfaces have low surface recombination velocities (*S*) but rapidly form a disordered oxide layer when exposed to air. This silicon/native silicon oxide interface displays high charge carrier surface recombination velocities (*S*), reflecting a significant density of electrically active trap sites.[1] These surfaces are of great importance because as electronic devices fabricated from Si become smaller in size, the properties of the semiconductor surface begin to dominate the properties of the device as a whole. Hence, there has been considerable interest in learning how to control surface properties through chemical methods. These protection strategies should prevent extensive oxidation of the Si(111) surface while preserving the low surface recombination velocity of the H-terminated Si(111) surface.

One promising technique that has received recent attention is the formation of surficial Si−C bonds.[2] To this end, the H-terminated Si surfaces of both single-crystal and porous Si substrates have been alkylated using alkylmagnesium reagents,[3,4] and halogenated surfaces have been alkylated using alkylmagnesium or alkyllithium reagents.[5−10] Alkylation has also been accomplished through free-radical initiation methods such as irradiating with ultraviolet light,[9,11−14] chemical free-radical activation,[15,16] thermal activation,[16−22] or hydrosilylation.[23−27] Other methods involve the formation of dangling Si surface bonds using scanning tunneling microscopy (STM) techniques[28] or the transition metal-catalyzed reduction of a terminal alkene directly on the Si−H surface.[29] Additionally, several electrochemical functionalization methods[30−35] have been described.

Previous work in our laboratory has shown that a two-step chlorination/alkylation technique passivates crystalline Si(111) surfaces toward both chemical oxidation and electron−hole recombination.[1,5] In the work described here, Si(111) surfaces were modified with straight-chain alkyl groups by four functionalization techniques: (i) chlorination/alkylation with either PCl_5 as the chlorinating agent or (ii) Cl_2(g) as the chlorinating agent, (iii) Lewis acid-mediated reduction of a terminal alkene, and (iv) electrochemical oxidation of CH_3MgI. The functionalized surfaces were initially characterized by X-ray photoelectron spectroscopy (XPS), and time-resolved radio frequency (rf) photoconductivity methods were used to determine the recombination velocities of charge carriers on the functionalized surfaces while the sample was maintained under N_2(g). XP spectra and surface recombination velocities were then measured periodically, while the functionalized surfaces were exposed to air for over 600 h. The chemical response of the surface to air exposure, determined by XPS, was correlated to the *S* values of the surface, to determine if changes in the surface recombination velocity could be linked to changes in the chemical composition of the functionalized Si surfaces.

II. Experimental Section

(A) Materials and Methods. *(1) Materials.* Two different types of Si(111) wafers were used in this study. The n-type

* Author to whom correspondence should be addressed.

10.1021/jp0222752 CCC: $25.00
Published on Web 05/20/2003

Si(111) wafers used for XPS measurements were polished only on one side and were obtained from Crysteco (Wilmington, OH). These samples were 525 μm thick and P-doped, with a resistivity of 2−8.5 Ω cm. Samples for surface recombination velocity measurements were obtained from Topsil Inc. (Frederikssund, Denmark). These wafers were float-zone grown n-type, P-doped, Si(111), 280 μm thick, with resistivities of 3500−6500 Ω cm, and were polished on both sides. The manufacturer reported a bulk charge carrier lifetime, τ_b, of 2 ms.

All solvents used in functionalization reactions were anhydrous, stored under N_2(g), and apart from occasionally pouring over molecular sieves, were used as received from Aldrich Chemical Corp. Solvents were only exposed to the atmosphere of a N_2(g)-purged flush box. Nanopure 18 MΩ cm resistivity H_2O was used at all times. All other chemicals were used as received unless otherwise specified.

(2) Sample Preparation. Before use, all wafers were chemically oxidized in 3:1 (v/v) concentrated H_2SO_4:30% H_2O_2(aq) at 100 °C for 1 h, rinsed in H_2O, and dried under a stream of N_2(g). Oxidized samples of approximately 1 cm^2 were cleaned by sonicating for 5 min in H_2O, rinsing with CH_3OH and acetone, sonicating for an additional 5 min in H_2O, and drying under a stream of N_2(g). Samples were etched for 20 min in 40% NH_4F(aq) (Transene Inc.) to produce a H-terminated Si surface. During the etching process the wafers were occasionally agitated to remove bubbles that formed on the surface. The samples were removed from the etching solution, rinsed in H_2O, dried under a stream of N_2(g), and immediately inserted via a quick-entry load lock into an ultrahigh vacuum (UHV) system for XPS measurements. The UHV chamber was connected via a second quick-entry load lock to a N_2(g)-purged flush box in which further surface modification reactions were conducted. Once a sample entered the UHV system it was not exposed to ambient air until after surface modification. Occasionally wafers were inserted directly into the vacuum-sealed antechamber of the N_2(g)-purged flush box to prevent scratches on the surface that arose from contact with the XPS sample holder.

(3) Functionalization by Chlorination/Alkylation. Chlorinated Si(111) surfaces were prepared by two different methods. In one chlorination method, a H-terminated sample was immersed into a saturated solution of PCl_5 in C_6H_5Cl that contained a few grains of $C_6H_5OOC_6H_5$ to act as a radical initiator.[5,6] The reaction solution was heated to 90−100 °C for 45 min. Samples were then removed from the reaction solution and rinsed in tetrahydrofuran (THF) followed by a rinse in CH_3OH and were then dried under a stream of N_2(g). Samples were occasionally also rinsed in 1,1,1,-trichloroethane (TCE) before drying under N_2(g).

In the second chlorination method, a H-terminated sample was placed into a Schlenk reaction tube and transported to a vacuum line. Approximately 50−200 Torr of Cl_2(g) (Matheson, 99.999%) was introduced through the vacuum line into the reaction tube, and the sample was illuminated for 30 s with 366 nm ultraviolet light from a UVP-type multiband lamp.[9,10] Rigorous exclusion of ambient air from the reaction tube was required to produce oxide-free surfaces. Excess Cl_2(g) was then removed under vacuum, and the flask was transported to the N_2(g)-purged flush box. XP spectra and surface charge carrier recombination velocities were collected for Cl-terminated samples that had been prepared through both chlorination routes.

The chlorine-terminated Si surfaces were alkylated by immersion in 1.0−3.0 M $C_nH_{2n+1}MgX$, where n = 1, 2, 6, 8 and X = Cl or Br, in either diethyl ether or THF (Aldrich). The reaction was performed for 1.5−16 h at 70−80 °C with longer alkyl chain lengths requiring the longer reaction times. Excess THF was added to all reaction solutions for solvent replacement. At the end of the reaction time, samples were removed from the reaction solution and were then rinsed in THF, CH_3OH, and occasionally TCE. Samples were then sonicated for 5 min each in CH_3OH and CH_3CN and were dried under a stream of N_2(g). After functionalization, XP spectra and charge carrier recombination velocities of these surfaces were collected under N_2(g). Occasionally a small Mg signal that presumably arose from the Grignard reagent appeared in the initial XP spectrum. When this peak was observed, the sample was sonicated in CH_3OH for an additional 10 min to remove any remaining Mg. The samples were then exposed to laboratory air, and XPS and rf photoconductivity data were collected periodically during air exposures of >600 h.

(4) Lewis Acid-Mediated Terminal Alkene Reduction. A third functionalization route employed in this study was the Lewis acid-catalyzed reduction of a terminal alkene directly on the H-terminated Si(111) surface. The alkenes 1-hexene and 1-octene (>94%, Aldrich) were filtered over activated alumina and were dried by refluxing over sodium/benzophenone. The alkenes were then transferred into the N_2(g)-purged flush box. Freshly etched, H-terminated Si(111) surfaces were functionalized by immersion in approximately equal volumes of the alkene and 1.0 M $C_2H_5AlCl_2$ in hexanes (Aldrich) at room temperature for 12 h.[24,25] Samples were removed from solution and were rinsed in THF, CH_2Cl_2, and CH_3OH, respectively, and were then dried under a stream of N_2(g). XP spectra and surface recombination velocities were then recorded on the functionalized surfaces. Data on these surfaces were first collected under a N_2(g) ambient, and samples were then exposed to air for extended periods of time during which XP spectra and rf photoconductivity decay data were periodically collected.

(5) Electrochemical Reduction of CH_3MgI. H-terminated Si(111) surfaces were also functionalized through the electrochemical oxidation of CH_3MgI.[32,33] Samples that were polished and functionalized on both sides were used to obtain both XP spectra and surface charge carrier recombination velocities for this system. These samples were treated slightly differently from those functionalized through the methods described above because of the need to protect the electrical contacts from the methylmagnesium iodide solution. A Teflon two-chambered cell was fabricated so that both sides of the double-polished wafer could be exposed to the electrolysis solution. Oxidized wafers were cleaned by rinsing with H_2O, CH_3OH, acetone, CH_3OH, and H_2O, respectively, and the samples were then dried under a stream of N_2(g). Dried samples were then mounted into the cell to perform the surface functionalization reactions. Ohmic contacts were made with Ga/In eutectic on the regions of the wafer that were exposed above and below the cell body, and the contacts were shorted together using a tinned Cu wire.

The sample was etched by filling both sides of the cell with 40% NH_4F(aq). After 20 min, the etching solution was removed and the cell was filled with H_2O to rinse the sample surface. The H_2O was then removed from the cell, and the sample was dried under a stream of N_2(g). The surface and interior of the cell could not be dried completely in a short period of time, so the partially dried sample was immediately placed into the antechamber of a N_2(g)-purged flush box and vacuum was applied to remove any remaining H_2O. The cell was then moved into the N_2(g)-purged flush box for electrochemical modification. Each chamber of the electrochemical cell contained a section of Cu gauze that served as a counter electrode. Both

pieces of Cu gauze were connected together using a Cu wire, thereby forming a single counter electrode.

Alkylation was performed in 3.0 M CH_3MgI in diethyl ether (Aldrich) by applying 0.1 mA cm^{-2} of constant anodic current density for 5 min with continuous stirring of the solution. After surface modification, the cell was rinsed with CH_2Cl_2 and CH_3OH, respectively. The cell was then dismantled, and the top and bottom ohmic contacts were scribed off to leave behind only the portion of the wafer that had been exposed to the reaction solution. This wafer was rinsed further in CH_3OH, sonicated in CH_3OH, further sonicated in CH_3CN, and dried with a stream of N_2(g). XP spectra and rf photoconductivity decay data were measured on this functionalized surface, and the sample was then exposed to air and monitored periodically for its surface composition and electrical properties.

(B) Instrumentation. *(1) XPS Measurements.* XP spectra were collected in a UHV chamber that has been described elsewhere.[5,36] The UHV chamber was maintained at a pressure of 10^{-10} Torr, although during sample analysis the pressure in the chamber rose to approximately $10^{-8}-10^{-9}$ Torr. X-rays of energy 1486.6 eV from the Al Kα line were incident onto the surface at an angle of 35° from the surface plane. Photoelectrons were collected by a hemispherical electron energy analyzer that was located 35° off the sample surface. The samples were conducting at room temperature, so no compensation for surface charging effects was necessary. Data were collected with the M-Probe ESCA Software version S-Probe 1.36.00. An initial survey scan was run from 0 to 900 or from 0 to 1000 BeV (binding electron Volts) to identify all chemical species on the surface. A second scan was collected at the Si 2p region at approximately 98.5−105.5 BeV to measure the presence of any SiO_2 species at 103.4 BeV. Wafers were fixed to the XPS sample holder at their edges, and XPS data were collected near the middle of the wafer to prevent interference from any surface oxide growth that might be promoted by scratches caused by contact with the sample fixture during handling of the sample.

The surface coverages of species of interest were compared between different samples by referencing all peaks to the Si 2p peak at 99.4 BeV. The area under the peaks obtained in the initial survey scan was determined by the XPS software. The detailed scan of the Si 2p region was used to determine the amount of Si oxides present. The Si $2p_{1/2}$ and Si $2p_{3/2}$ peaks were fitted with two peaks held 0.60 BeV apart and with the Si $2p_{1/2}$:Si $2p_{3/2}$ peak area ratio maintained at 0.51, as has been described previously.[5,36] Any peak detected between 100 and 104 BeV, where $Si^{+}-Si^{4+}$ oxides would be located, was fitted to a third peak.[37] Peak line shapes were set at 95% Gaussian and 5% Lorentzian, with a 15% asymmetry. The SiO_x:Si 2p peak area ratio was then obtained from the area under the third curve divided by the total area of the Si $2p_{1/2}$ and Si $2p_{3/2}$ peaks. This peak area corresponds to the coverage of Si^{+}, Si^{2+}, Si^{3+}, and Si^{4+} oxides on the surface.

The equivalent fractional monolayer coverage of SiO_x on the Si(111) substrate was determined from the SiO_x:Si 2p peak area ratio using a substrate-overlayer model.[36,38] The overlayer thickness, d_{ov}, was computed using

$$d_{ov} = \lambda_{ov} \sin\theta \left\{ \ln\left[1 + \left(\frac{I^0_{Si}}{I^0_{ov}} \right) \left(\frac{I_{ov}}{I_{Si}} \right) \right] \right\} \qquad (1)$$

where λ_{ov} is the attenuation factor of the overlayer (2.6 nm), θ is the electron takeoff angle relative to the sample surface (35° for this instrument), I^0_{Si}/I^0_{ov} is an instrument normalization factor related to the sensitivity and abundance of the substrate and overlayer species, determined to be 1.3 for this instrument for a SiO_2 overlayer on a Si substrate, and I_{ov}/I_{Si} is the measured SiO_2:Si 2p peak area ratio. Assuming that the oxide is composed entirely of SiO_2, the computed overlayer thickness, d_{ov}, was divided by the thickness of a monolayer of SiO_2, 0.35 nm, to determine the equivalent fractional monolayer of SiO_2 present.[36]

For very thin oxide overlayers, the monolayer coverage of oxidized Si can also be calculated directly from the SiO_x:Si 2p peak area ratio.[36] This approach directly determines the amount of oxidized Si present on the surface regardless of whether it is SiO_2 or is composed of other oxides of Si. The total observed Si 2p signal is

$$I_{Si} \approx n_{Si}\sigma_{Si}\int_0 \exp(-z/I_{Si})\, dz = n_{Si}\sigma_{Si}l_{Si} \qquad (2)$$

where n_{Si} is the atomic number density of Si atoms (5.0×10^{22} atoms cm^{-3}), σ_{Si} is the atomic photoionization cross-section of Si, and the escape depth, l_{Si}, is given by

$$l_{Si} = \lambda_{Si} \sin\theta \qquad (3)$$

with $\lambda_{Si} = 1.6$ nm. The measured signal arising from the oxidized surface Si atoms at higher binding energies than the bulk Si 2p peak is given by

$$I_{Si,surf} = n_{Si,surf}\sigma_{Si} \qquad (4)$$

where $n_{Si,surf}$ is the surface density of Si atoms, 7.8×10^{14} atoms cm^{-2} for Si(111). If every surface Si atom is oxidized, then the relative intensity of the oxidized Si peak to bulk Si peak can be found by combining eqs 2 and 4:

$$\frac{I_{Si,surf}}{I_{Si,bulk}} = \frac{n_{Si,surf}\sigma_{Si}}{n_{Si}\sigma_{Si}l_{Si} - n_{Si,surf}\sigma_{Si}} = \frac{n_{Si,surf}}{n_{Si}l_{Si} - n_{Si,surf}} \qquad (5)$$

As can be seen in eq 5, the SiO_x:Si 2p peak area ratio is independent of the photoionization cross-section of all species present in the scan. Substituting into eq 5 yields a ratio of 0.21 for a Si(111) surface on which 100% of the surface Si atoms are oxidized. The observed oxidized/bulk Si 2p peak area ratios were therefore divided by this normalization constant to estimate the fraction of surface atoms that were oxidized.

(2) Surface Recombination Velocity Measurements. Charge carrier lifetimes were measured using a contactless time-resolved rf conductivity apparatus.[1] Samples were illuminated at 1064 nm with 10 ns pulses from a Nd:YAG laser operating at a repetition rate of 10 Hz. To ensure high-level injection conditions, the pulse power was 7×10^{-4} mJ $pulse^{-1}$ cm^{-2}, which resulted in an injected carrier concentration in the semiconductor immediately after the light pulse of 4×10^{13} carriers cm^{-3}. The sample was placed over a coil emitting a 450 MHz rf signal which was absorbed by carriers in the semiconductor. The coil also collected and measured the amount of unabsorbed 450 MHz signal that was reflected back from the sample. The difference in intensity between the initial and reflected signal was proportional to the rf absorbed by the sample. Signals were averaged over 128 decays, plotted on a digital oscilloscope (Tektronix, TDS210), and captured by the PC data acquisition program WaveStar. Data were fitted to a single-exponential decay to determine τ, the lifetime of charge carriers in the semiconductor. Once samples were set in the rf conductivity sample holder, they were not handled again for the duration of the experiment to prevent scratching of the surface.

The fundamental charge carrier decay lifetime, τ, is dependent on the lifetime of the charge carriers both in the bulk and at the

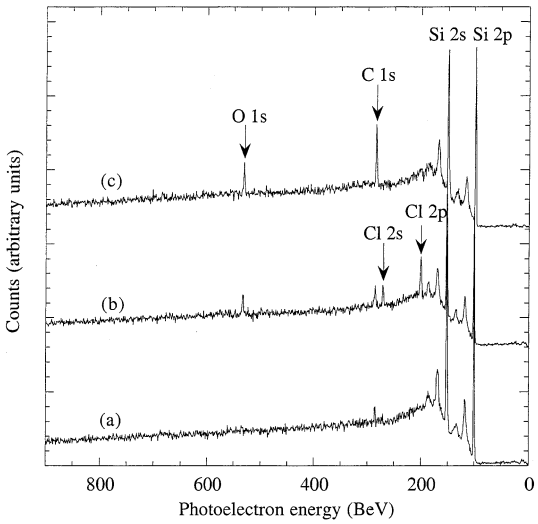

Figure 1. Survey scan XP spectra of a Si(111) surface (a) cleaned and etched in 40% NH_4F(aq) for 20 min, (b) chlorinated with saturated PCl_5 in chlorobenzene with $C_6H_5OOC_6H_5$ at 90−100 °C for 45 min, and (c) then alkylated with $C_8H_{17}MgCl$ for 16 h.

surfaces of the sample. The surface recombination velocity, *S*, can be related to the measured lifetime using

$$S = \frac{d}{2}\left(\frac{1}{\tau} - \frac{1}{\tau_b}\right) \tag{6}$$

where *d* is the sample thickness and τ_b is the lifetime of a charge carrier in the bulk of the semiconductor.[1] When $\tau_b \gg \tau$, the expression for *S* reduces to

$$S = d/2\tau \tag{7}$$

III. Results

(A) Surfaces Functionalized by Chlorination/Alkylation Methods. *(1) XPS Data.* Figure 1 presents representative XPS data for the functionalization of Si(111) surfaces using a two-step chlorination/alkylation route. As has been shown previously,[5,9,10] on a freshly etched Si(111) surface (Figure 1a), only Si 2p and Si 2s peaks, at 100 BeV and 150 BeV, respectively, were observed. After chlorinating the surface in a solution of PCl_5, Cl 2p (200 BeV) and Cl 2s (270 BeV) peaks became visible (Figure 1b). After alkylation, the Cl peaks disappeared and a significant C 1s peak appeared at 285 BeV (Figure 1c). Table 1 presents the peak area ratios of C, Cl, and O that were detected in these XPS scans.

The XPS peak for the Si^{4+} in SiO_2 appears at 4.3 BeV higher in energy than Si^0, so oxidation of the surface Si atoms is accompanied by the appearance of Si 2p peaks having energies > 100 BeV. No SiO_2 was observed in the high-resolution Si 2p XPS scans at any step in the alkylation process, indicating that the O 1s peak at 532 BeV shown in Figure 1 was due to the presence of small amounts of adventitious O on the surface.

Figure 2 presents high-resolution XPS scans of the Si 2p region during the air oxidation of H-terminated Si(111) surfaces. A freshly etched H-terminated Si(111) surface (Figure 2a) oxidized rapidly and displayed a prominent silicon oxide peak after only 4 h of exposure (Figure 2b). The oxide grew further upon extended exposure to air (Figure 2c,d). The SiO_x:Si 2p peak area ratio, corresponding to the measured ratio of oxidized to unoxidized surface Si, for H-terminated Si(111) is plotted in Figure 3. This ratio was used to compute the monolayer equivalents of SiO_2 on the surface (Table 2). After 216 h of exposure to ambient air, the H-terminated Si surface displayed 1.4 monolayer equiv of SiO_2 (Table 2). Similar oxidation behavior was observed for Cl-terminated surfaces that had been prepared using either chlorination procedure (Figure 3, Table 2). In contrast, CH_3-terminated surfaces that had been prepared through either chlorination route displayed negligible oxide growth after up to 50 h of air exposure (Figure 3). Even after >200 h in air, the CH_3-terminated surfaces displayed less oxide growth than was observed after a few minutes of air exposure of the H- or Cl-terminated Si(111) surfaces (Figure 3).

Similar behavior was observed for C_2H_5-terminated surfaces (Figure 4). Oxidation was suppressed on alkylated surfaces that had been prepared through use of either PCl_5 or Cl_2 as the chlorinating agent (Table 2). On all alkylated surfaces, silicon oxide growth was negligible for the first ≈30 h of the experiment, and after 200 h in air, only <0.9 equiv monolayers of SiO_2 were observed. As shown in Table 2, no clear difference in the rate of surface oxidation was observed as the chain length of the alkyl group increased.

TABLE 1: Normalized Peak Area Ratios for Species Present on the Functionalized Si(111) Surface

surface preparation route	-R	XPS peak area ratio[a] C 1s	O 1s	Cl 2p
PCl_5/ $C_nH_{n+1}MgX$	-Cl	0.3 ± 0.2	0.5 ± 0.2	0.45 ± 0.06
	$-CH_3$	0.52 ± 0.03	0.459 ± 0.003	
	$-C_2H_5$	0.40 ± 0.004	0.27 ± 0.07	
	$-C_6H_{13}$	0.68 ± 0.08	0.4 ± 0.1	
	$-C_8H_{17}$	0.6 ± 0.1	0.3 ± 0.2	
Cl_2(g)/ $C_nH_{2n+1}MgX$	-Cl	0.3 ± 0.2	0.2 ± 0.1	0.8 ± 0.4
	$-CH_3$	0.62 ± 0.9	0.75 ± 0.8	
	$-C_2H_5$	0.36 ± 0.06	0.3 ± 0.1	
	$-C_8H_{17}$	0.75 ± 0.03	0.48 ± 0.04	
C_nH_{2n+1}-CH=CH_2/ $C_2H_5AlCl_2$	$-C_6H_{13}$ control[b]	0.17 ± 0.01	0.21 ± 0.02	
	$-C_8H_{17}$ control[b]	0.26 ± 0.01	~0.1	
	$-C_6H_{13}$	0.46 ± 0.08	~0.1	
	$-C_8H_{17}$	0.6 ± 0.1	0.247 ± 0.002	
CH_3MgI/h^+	$-CH_3$	1.4 ± 0.9	1.3 ± 0.7	

[a] Values are normalized to the Si 2p peak area. [b] Surface prepared by immersing the sample in alkene without $C_2H_5AlCl_2$.

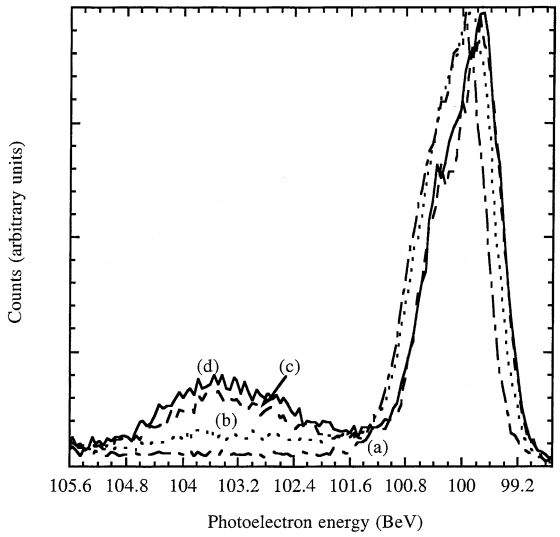

Figure 2. High-resolution XP spectra of the Si 2p region of a H-terminated Si(111) surface that was (a) freshly etched (dashed−dotted line) and then exposed to ambient laboratory air for (b) 4 h (dotted line), (c) 72 h (dashed line), and (d) 216 h (solid line).

TABLE 2: Normalized SiO_x:Si 2p Peak Area Ratio and Fractional Monolayer Coverage of SiO_x on the Functionalized Si(111) Surface

		XPS SiO_x:Si equiv monolayer coverage			
surface preparation route	-R	time in air (h)	SiO_x:Si 2p peak area ratio	equiv monolayers of SiO_2[a]	equiv monolayers of SiO_x[b]
NH_4F etch	-H	216	0.3	1.4	1.4
$PCl_5/C_nH_{2n+1}MgX$	-Cl	264	0.40 ± 0.09	1.8 ± 0.3	1.9 ± 0.4
	$-CH_3$	216	0.16 ± 0.08	0.8 ± 0.4	0.8 ± 0.4
	$-C_2H_5$	216	0.17 ± 0.03	0.9 ± 0.1	0.8 ± 0.1
	$-C_6H_{13}$	192	0.18 ± 0.02	0.90 ± 0.07	0.86 ± 0.07
	$-C_8H_{17}$	192	0.12	~0.6	~0.6
$Cl_2(g)/C_nH_{2n+1}MgX$	-Cl	215	0.306 ± 0.009	1.43 ± 0.04	1.46 ± 0.04
	$-CH_3$	288	0.11	~0.6	~0.5
	$-C_2H_5$	312	0.08 ± 0.02	0.44 ± 0.09	0.40 ± 0.08
$C_nH_{2n+1}CH{=}CH_2/C_2H_5AlCl_2$	$-C_6H_{13}$ control[c]	192	0.281 ± 0.008	1.33 ± 0.03	1.34 ± 0.04
	$-C_8H_{17}$ control[c]	192	0.24 ± 0.01	1.17 ± 0.05	1.16 ± 0.06
	$-C_6H_{13}$	168	0.4 ± 0.2	1.6 ± 0.7	1.7 ± 0.9
	$-C_8H_{17}$	360	0.21 ± 0.02	1.01 ± 0.07	0.98 ± 0.07

[a] Calculated from eq 1 and then divided by 0.35 nm. [b] Calculated by dividing the SiO_x:Si 2p peak area ratio by 0.21, a normalization constant representing 1 fractional monolayer of SiO_x calculated from eq 5. [c] Surface prepared by immersing the sample in alkene without $C_2H_5AlCl_2$.

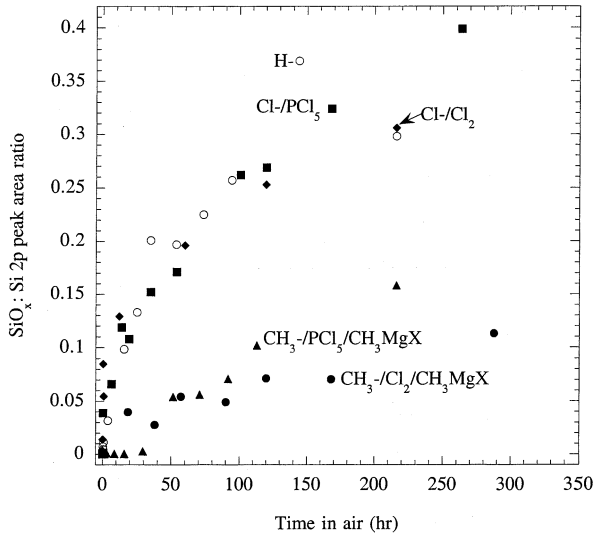

Figure 3. Ratio of the oxidized Si 2p peak area to the bulk Si 2p peak area for Si(111) surfaces exposed to ambient air over extended time periods: open circles, H-terminated Si; squares, Cl-terminated Si prepared using PCl_5; diamonds, Cl-terminated Si prepared using Cl_2-(g); triangles, CH_3-terminated surface prepared through PCl_5/CH_3MgCl; closed circles, CH_3-terminated surface prepared through $Cl_2(g)/CH_3$-MgBr. Although the standard deviation of oxide growth was sometimes large, occasionally as much as 50% of the value, no overlap of the standard deviation of H- and Cl-terminated surfaces and the CH_3-terminated surfaces was observed after 30 h in air.

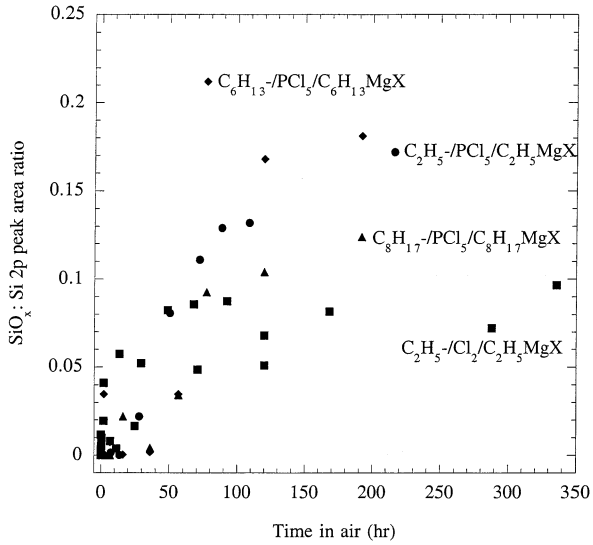

Figure 4. Ratio of the oxidized Si 2p peak area to the bulk Si 2p peak area for alkylated Si(111) prepared through chlorination/alkylation while exposed to ambient air over extended time periods: circles, C_2H_5-terminated Si prepared through PCl_5/C_2H_5MgBr; squares, C_2H_5-terminated Si prepared through $Cl_2(g)/C_2H_5MgBr$; diamonds, C_6H_{13}-terminated Si prepared through $PCl_5/C_6H_{13}MgBr$; triangles, C_8H_{17}-terminated Si prepared through $PCl_5/C_8H_{17}MgCl$. Standard deviations were large (~50%), and no significant difference was observed for the different chain lengths.

(2) Surface Recombination Velocities. Table 3 summarizes the rf photoconductivity decay data for the various surfaces of interest. Silicon surfaces that had been functionalized through the chlorination/alkylation route displayed long charge carrier lifetimes and low surface recombination velocities.[1] Methyl-terminated Si surfaces that were prepared using either chlorination method displayed the lowest charge carrier recombination velocity of the chain lengths included in this study. After methyl-terminated surfaces were exposed to laboratory air, the carrier lifetime increased over a period of ~24 h, after which it remained stable for the duration of the experiment (150−700 h). The CH_3-terminated surfaces prepared from a PCl_5-chlorinated surface exhibited a stabilized *S* value of 80 ± 30 cm s^{-1}, and surfaces prepared from $Cl_2(g)$ followed by treatment with CH_3MgBr exhibited a stabilized *S* value of 150 ± 60 cm s^{-1}. Ethyl-terminated Si surfaces functionalized through both chlorination techniques behaved similarly, with stabilized *S* values of 80 ± 20 and 200 ± 80 cm s^{-1} for the PCl_5/C_2H_5-MgBr- and $Cl_2(g)/C_2H_5MgBr$-treated surfaces, respectively. These values of *S* indicate that these two alkylation techniques produced passivated surfaces that maintained low electrically active trap densities for extended periods of time in air.

In general, the *S* values of all of the alkylated surfaces were similar to each other. However, somewhat more complex behavior was observed on surfaces prepared using PCl_5/C_6H_{13}-MgBr or $PCl_5/C_8H_{17}MgCl$, as shown in Figure 5. Under $N_2(g)$, the rf photoconductivity decay lifetimes were 80 ± 50 and 80 ± 20 μs for the C_6H_{13}- and C_8H_{17}-terminated surfaces, respectively. After 24 h of exposure to air, the lifetimes decreased to 60 ± 30 and 50 ± 10 μs, respectively. Upon extended air exposure, however, the lifetimes gradually rose over a period of 600−700 h to 120 ± 20 and 150 ± 7 μs, at which point the experiment was terminated.

A series of controls was run to determine if the observed lifetimes were the result of experimental conditions and not bonded alkane chains. Freshly etched, H-terminated Si(111)

TABLE 3: Charge Carrier Lifetimes and Recombination Velocities of Functionalized Si(111) Surfaces

		time in air					
		0 min (under N_2(g))		10 min		>24 h	
surface preparation route	-R	τ (μs)	S (cm s^{-1})	τ (μs)	S (cm s^{-1})	τ (μs)	S (cm s^{-1})
NH_4F(aq)	-H, control[a]	11.8 ± 0.6	1180 ± 60	<10	>1400	<10	>1400
	-H, control[b]	10 ± 1	1350 ± 10	<10	>1400	<10	>1400
	-H, control[c]	21.5 ± 0.4	650 ± 10			<10	>1400
$PCl_5/C_nH_{2n+1}MgX$	-Cl	510 ± 140	28 ± 8	300 ± 30	46 ± 4	<10	>1400
	-Cl, control[d]	70 ± 6	200 ± 20	40 ± 20	370 ± 140	<10	>1400
	-CH_3	130 ± 60	130 ± 50	140 ± 30	100 ± 20	200 ± 70	80 ± 30
	-C_2H_5	40 ± 20	450 ± 180	70 ± 50	260 ± 100	200 ± 90	80 ± 20
	-C_6H_{13}	80 ± 50	260 ± 140	60 ± 30	270 ± 110	120 ± 20	120 ± 20
	-C_8H_{17}	80 ± 20	190 ± 50	50 ± 10	280 ± 60	150 ± 7	93 ± 4
Cl_2(g)/$C_nH_{2n+1}MgX$	-Cl	460 ± 110	31 ± 7	370 ± 70	39 ± 7	<10	>1400
	-CH_3	70 ± 20	250 ± 150	50 ± 20	330 ± 230	110 ± 30	150 ± 60
	-C_2H_5	31 ± 7	470 ± 100	37 ± 8	400 ± 100	80 ± 30	200 ± 80
$C_nH_{2n+1}CH{=}CH_2/C_2H_5lCl_2$	-C_6H_{13}	40 ± 10	410 ± 120	23 ± 7	660 ± 190	<15	>1200
	-C_6H_{13}, control[e]	<10	>1400			<10	>1400
	-C_8H_{17}	20 ± 10	690 ± 270	18 ± 4	790 ± 160	<15	>1200
	-C_8H_{17}, control[e]	<10	>1400			<10	>1400
CH_3MgI/h^+	-CH_3	18 ± 6	860 ± 200			40 ± 20	460 ± 200
	-CH_3, control[f]	<10	>1400			<10	>1400

[a] Control surfaces prepared by immersing a H-terminated surface in chlorobenzene and heating for the appropriate reaction time. [b] Control surfaces prepared by immersing a H-terminated surface in chlorobenzene, followed by immersion in THF and heating for the appropriate reaction times in each solvent. [c] Control surfaces prepared by immersing a H-terminated surface in chlorobenzene with benzyl peroxide and heating for the appropriate reaction time. [d] Control surfaces prepared by immersing a Cl-terminated surface in THF at 70−80 °C for 3.5 h. [e] Control surfaces prepared by immersing a H-terminated surface in alkene without $C_2H_5AlCl_2$ for 12 h at room temperature. [f] Control surface prepared by immersing a H-terminated surface in CH_3MgI without passing current.

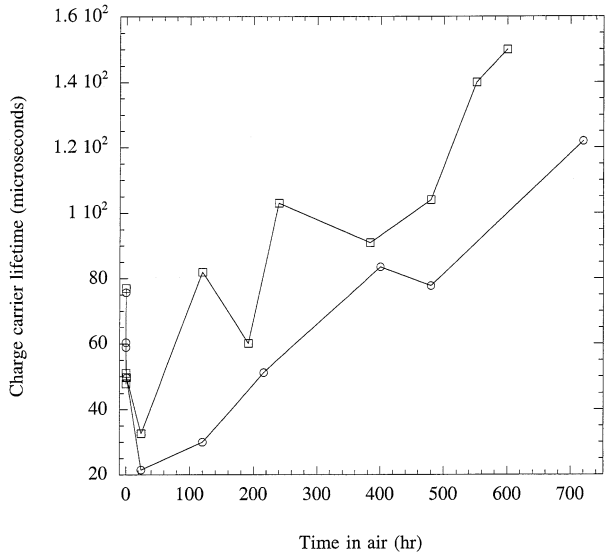

Figure 5. Charge carrier lifetimes of C_6H_{13}- and C_8H_{17}-terminated Si(111) prepared by exposure to PCl_5 followed by reaction with alkylmagnesium halide: circles, C_6H_{13}-terminated Si(111); squares, C_8H_{17}-terminated Si(111).

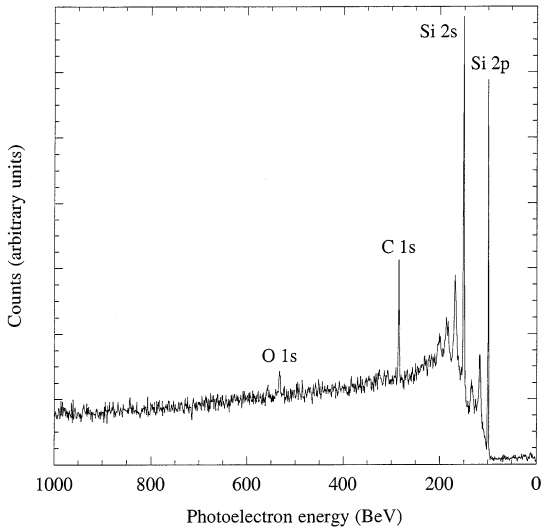

Figure 6. Survey scan XP spectrum of C_6H_{13}-terminated Si(111) prepared by reduction of 1-hexene catalyzed by $C_2H_5AlCl_2$.

samples that were immersed in either chlorobenzene, chlorobenzene and benzyl peroxide, or chlorobenzene followed by THF and heated for identical reaction times as the functionalized surfaces displayed short charge carrier lifetimes indicative of highly defective surfaces (Table 3). Charge carrier lifetimes for these control surfaces were <22 μs (S = 650 cm s^{-1}) under N_2(g) and decreased to <10 μs after 1−3 h of exposure to laboratory air. Cl-terminated Si(111) surfaces prepared by either chlorination method displayed charge carrier lifetimes of ≈500 μs (S = 30 cm s^{-1}) under N_2(g), but τ decreased to ≈300 μs after only 10 min in air, and surface-limited carrier lifetimes, with τ < 10 μs (S > 1400 cm s^{-1}), were observed after 24 h in air. Surface recombination velocities of Cl-terminated Si(111) samples prepared by chlorination with PCl_5 that had been immersed in THF at 70−80 °C for 3.5 h were 200 ± 20 cm s^{-1} under N_2(g) but increased to S > 1400 cm s^{-1} after 24 h of exposure to ambient air.

(B) Lewis Acid-Mediated Terminal Alkene Reduction. *(1) XPS Results.* Figure 6 displays the XP spectrum of a freshly prepared C_6H_{13}-terminated surface that was prepared through the Lewis acid-catalyzed reduction of 1-hexene. The C 1s peak area was somewhat lower than that observed for hexyl-terminated surfaces that had been prepared through the PCl_5 chlorination/$C_6H_{13}MgBr$ alkylation route (0.46 ± 0.08 vs 0.68 ± 0.08) (Table 1). Octyl-terminated surfaces, however, displayed the same C 1s surface coverages for this method and for the chlorination/alkylation route. Control surfaces prepared by immersing Si(111) samples in either 1-hexene or 1-octene for 12 h without addition of the Lewis acid catalyst showed much lower normalized C 1s and O 1s peak area ratios (Table 1),

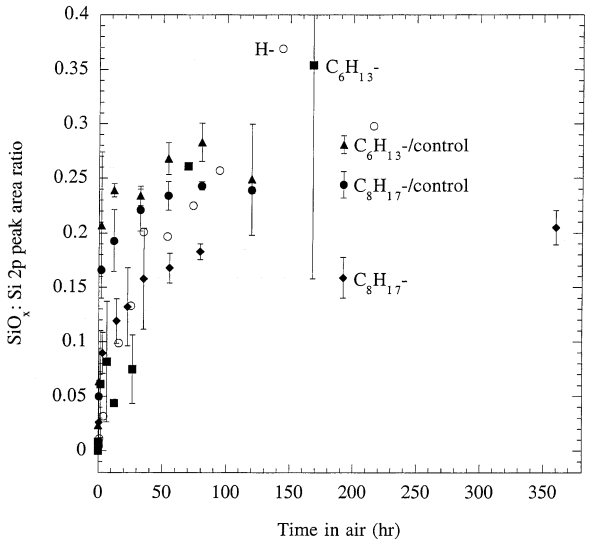

Figure 7. Ratio of the oxidized Si 2p peak area to the bulk Si 2p peak area for Si(111) surfaces prepared by terminal olefin reduction catalyzed by $C_2H_5AlCl_2$ and exposed to ambient air over extended time periods: open circles, H-terminated Si; squares, C_6H_{13}-terminated Si; diamonds, C_8H_{17}-terminated Si; triangles, control surface immersed in 1-hexene with no Lewis acid; closed circles, control surface immersed in 1-octene with no Lewis acid.

indicating that functionalization did not readily occur in the absence of the catalyst.

Figure 7 summarizes the Si 2p high-resolution XPS oxidation data for C_6H_{13}- and C_8H_{17}-terminated Si(111) surfaces prepared through this functionalization route, and also displays the results for surfaces that had been prepared by immersing a sample into the terminal olefin without addition of the $C_2H_5AlCl_2$ catalyst. The C_6H_{13}-terminated surface behaved identically to both of the controls and to the H-terminated surface, indicating that this functionalization technique did not suppress the rate of oxidation of the Si. While all of the surfaces functionalized through a two-step chlorination/alkylation process fully resisted oxidation for the first 30 h in air, the C_6H_{13}- and C_8H_{17}-terminated surface prepared through reduction of a terminal olefin displayed rapid oxidation behavior identical to the H-terminated Si(111) surfaces. Functionalization with C_8H_{17} groups provided some improved long-term resistance to oxidation. After 200 h in air, the C_8H_{17}-functionalized surface displayed a normalized SiO_x:Si 2p peak area ratio of 0.21, as compared to a SiO_x:Si 2p peak area ratio of 0.12 observed for an octyl-terminated surface prepared by PCl_5 chlorination/$C_8H_{17}MgCl$ alkylation.

(2) Surface Charge Carrier Recombination Results. Table 3 presents the *S* values of C_6H_{13}- and C_8H_{17}-terminated Si(111) that had been functionalized by the Lewis acid-catalyzed reduction of the terminal alkene. Under a N_2(g) ambient, the initial charge carrier lifetimes of these surfaces were 20−40 μs, but the lifetimes decayed rapidly upon exposure to air, with $\tau < 15$ μs after 24 h of air exposure. Unlike the lifetimes of hexyl- and octyl-terminated Si(111) surfaces prepared through the $PCl_5/C_nH_{2n+1}MgX$ route, which dropped upon exposure to air but recovered their initial values over a period of 600−700 h, the lifetimes of hexyl- and octyl-functionalized Si(111) surfaces prepared through the reduction of a terminal olefin did not recover and remained <15 μs until the experiment was terminated (≈500 h). Surface recombination velocities on control surfaces prepared by immersion in terminal alkene without the catalyst were >1400 cm s^{-1} (Table 3), indicative of a highly defective surface containing a large number of electrical recombination sites.

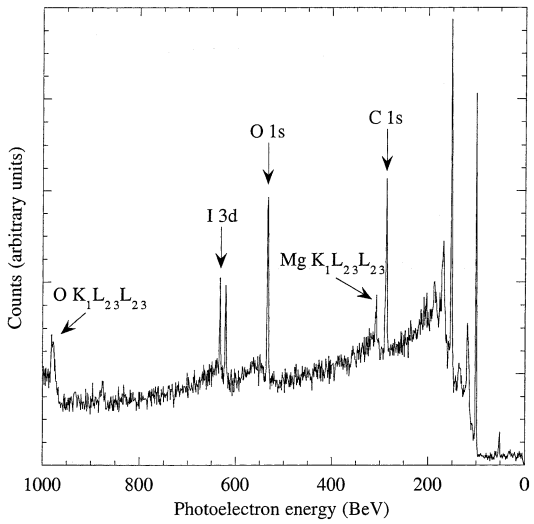

Figure 8. Survey scan XP spectrum of CH_3-terminated Si(111) prepared by anodic grafting in CH_3MgI in diethyl ether.

(C) Electrochemical Reduction of CH_3MgI. *(1) XPS Results.* Figure 8 displays the XP spectra of functionalized Si(111) surfaces prepared by anodization in 3.0 M CH_3MgI in diethyl ether. A large C 1s peak was observed at 285.5 BeV with a C 1s:Si 2p peak area ratio of 1.4 ± 0.9. Large peaks were also observed at 532 and 980 BeV, corresponding to the O 1s and O $K_1L_{23}L_{23}$ (Auger) peaks, respectively. Peaks at 620 and 631 BeV, identified as I $3d_{5/2}$ and I $3d_{3/2}$, respectively, were also observed periodically. Occasionally a peak at 307 BeV, tentatively identified as the Mg $K_1L_{23}L_{23}$ peak, was also observed, even after the samples had been sonicated extensively in CH_3OH and CH_3CN.

The magnitude of the C 1s:Si 2p peak area ratio was larger than that expected for alkyl chains of at least 12 carbon atoms in length,[5] indicating that the C 1s signal was not due entirely to surface-bonded methyl groups. The O 1s:Si 2p peak ratio (Table 1) was substantially larger than that observed for any other alkylation method studied in this work, although no SiO_x signals were observed in the spectra of freshly prepared CH_3-terminated surfaces.

Methylated samples were kept in air for up to 150 h and XPS data were again collected on the surfaces. All surfaces showed a SiO_x:Si 2p normalized peak area ratio of >0.1, although the peak areas varied widely and were occasionally in excess of 0.4. This latter value corresponds to an equivalent SiO_2 coverage of at least 2 monolayers.

(2) Surface Recombination Velocity Data. After an extended period of time in air, τ values for these surfaces were 40 ± 20 μs ($S = 460 \pm 200$ cm s^{-1}, Table 3). A control surface was formed by immersing the Si electrode and the Cu counter electrode into the CH_3MgI solution while no current was passed through the cell. The resulting surface exhibited $\tau \leq 10$ μs over a period of 100 h in air, after which time the sample was discarded. The electrochemical functionalization method therefore produced a surface which was moderately more passivated electrically than a H-terminated Si(111) surface but which still possessed significant levels of electrically active surface recombination sites.

IV. Discussion

Alkylation using both of the chlorination/alkylation routes significantly reduced the rate of air oxidation and concomitantly preserved the electrical properties of the H-terminated Si surface. Although the two chlorination routes produced differing levels

of Cl on the Si(111) surface, subsequent alkylation resulted in very similar coverages of alkyl groups on the Si surface as determined by XPS (Table 1).

The degree of electrical passivation obtained through either chlorination/alkylation method is notable. The surface trap density, N_t, may be related to S through

$$S = N_t \sigma v_{th} \tag{8}$$

where σ is the cross-section for carrier capture on the surface, typically 10^{-15} cm^2, and v_{th} is the thermal charge carrier velocity, which is 5.2×10^6 cm s^{-1} in n-type Si(111) at room temperature.[1,39,40] Hence the observed S value for such surfaces, 200 cm s^{-1}, corresponds to $N_t = 4 \times 10^{10}$ cm^{-2}. Assuming a surface atom density of $\sim 10^{15}$ cm^{-2},[40] this corresponds to an electrically active defect density of only 1 atom in every 10^5 surface sites.

It is interesting to compare the behavior of methyl-terminated Si(111) surfaces to surfaces functionalized with longer alkyl chains. Because the distance between atop atoms on the unreconstructed Si(111) surface (3.8 Å)[40] is larger than the van der Waals radius of a methyl group (2.2 Å),[33] methyl groups are the only alkyl group that can terminate every Si atop atom site, and thus are unique among the straight-chain alkyls.[1] It therefore would be expected that methylated Si(111) surfaces would have the lowest incidence of defects and would display the lowest surface recombination velocities. This behavior was in fact observed experimentally, although surprisingly the other alkyl groups produced surfaces with S values that were only a factor of ~ 2 higher than those of the methylated Si(111) surface.

The chemical stability of the functionalized surfaces will reflect not only the degree of surface termination but also the nature of the alkylating agent, the ability of the overlayer to prevent oxidants from reaching the surface, the level of surface defects, and possibly other factors. For short term exposure to air, all of the surfaces prepared by the chlorination/alkylation routes were much more chemically inert to oxidation than the H-terminated or Cl-terminated Si(111) surfaces. Longer term exposure to air did produce some evidence for oxidation, although the levels of oxide never exceeded the equivalent of 1 monolayer of SiO_2 even after up to 300 h of air exposure. The methyl-terminated surfaces appeared to be somewhat more resistant to oxidation than surfaces alkylated with longer alkyl chains, which is consistent with the notion that CH_3 groups can terminate more Si atop sites with Si−C bonds and with the hypothesis that Si−C bonds are more kinetically inert to oxidative processes than are the unalkylated Si atop sites. It is possible that the greater incidence of pinhole defects in surfaces functionalized with longer alkyl chains is offset by the greater hydrophobicity of these chains, so that the overall rate of oxidation is similar for the surfaces functionalized with alkyl chains ranging from one to eight carbons in length.[22]

In some cases, the changes in surface composition correlated well with changes in the electrical properties of the surface, while in other cases the growth of oxide, surprisingly, did not degrade the electrical properties of the Si surface. The rapid oxide growth seen upon air exposure of the H- and Cl-terminated surfaces correlated with a precipitous drop in surface charge carrier lifetimes. However, the slower, yet still significant, oxide growth on the alkylated surfaces prepared through chlorination/alkylation techniques did not deleteriously affect the charge carrier lifetimes of such surfaces. In fact all of the samples that were functionalized using the chlorination/alkylation route showed an increased lifetime with longer exposure to air. A similar effect on stabilizing the photoluminescent behavior of porous Si modified with surface-bound organic functional groups has been described previously.[21,22] It is possible that slower growth of the oxide allows it to form in a more ordered fashion than rapid growth seen on the unpassivated surfaces and that this ordered oxide does not introduce electron−hole energy traps that promote extensive recombination. This is supported by the well-documented observation that high-quality SiO_2 layers grown by thermal annealing have low surface charge carrier recombination behavior but that the native oxide, grown in an uncontrolled fashion in air, supports high charge carrier recombination velocities.[21,22,41] Detailed spectroscopic studies are warranted to elucidate further the structure of the electronically passivated Si/Si oxide interface that is produced upon air oxidation of the alkylated Si(111) surface.

SCHEME 1

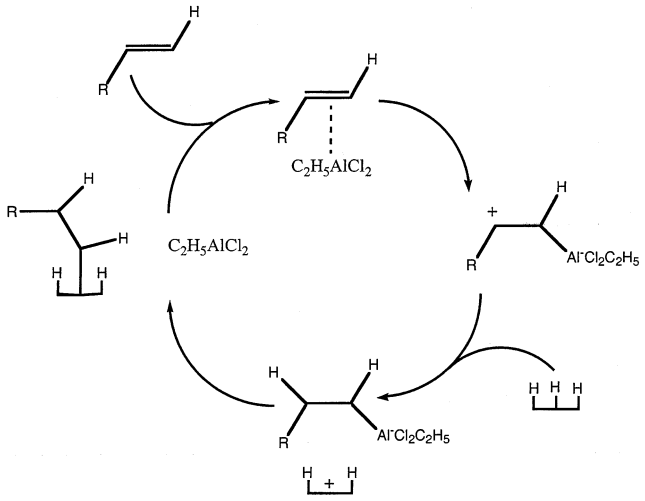

Alkylated surfaces produced by the Lewis acid-catalyzed reduction of a terminal alkene directly on the H-terminated surface showed significantly higher surface charge carrier recombination rates than those produced through the chlorination/alkylation processes. This observation can be understood when the probable mechanism of alkylation, shown in Scheme 1, is considered.[25,42,43] Because alkylation involves coupling between an alkyl bonded to the negatively charged Lewis acid catalyst and a hindered surface-localized cation, it is likely that steric constraints will prevent alkylation from occurring at all possible surface sites. This will result in a surface with substantial pinhole defects that is less protected from oxidation in air. This functionalization technique, as well as transition metal-catalyzed terminal alkene reductions, have been employed successfully on porous Si surfaces.[24,25,29] Differences in behavior of single-crystal and porous Si substrates may arise in part from the greater surface area of porous Si, which will present less steric resistance to coupling between the surface and the catalyst, as well as the distribution of chemically different silicon hydride sites that is present on porous Si surfaces relative to that of H-terminated Si(111) crystals. Clearly, the reaction chemistry of crystalline Si(111) is quite sensitive to the method of preparation of the alkyl overlayer on the functionalized Si surface.

Data from XPS and rf conductivity decay methods indicate that alkylated Si(111) surfaces formed by an electrochemical treatment are not as passivated chemically or electrically as surfaces that have been prepared through the chlorination/alkylation routes. Infrared spectroscopic studies have indicated that the electrochemical anodization method produces some degree of methylation of the Si(111) surface.[33] The XPS data

described above indicate however that this surface also has a large O 1s XPS signal, as well as signals from other elements used in the functionalization step. Accordingly, these surfaces displayed chemical and electrical properties inferior to any of the alkylated surfaces that were prepared by either of the chlorination/alkylation routes. Clearly, although all four of the Si surfaces studied in this work nominally had alkyl groups introduced onto the Si surface, subtle changes in the extent and quality of the alkyl termination are significant factors in determining the magnitude and degree of chemical and electrical passivation of the resulting functionalized Si surfaces.

V. Conclusions

Significant differences were observed in the chemical and electrical properties of Si(111) surfaces that were functionalized to introduce alkyl groups on the surface. A two-step functionalization route involving chlorination of a freshly etched H-terminated surface followed by alkylation with a Grignard reagent resulted in surfaces that resisted oxidation in air for a period of ≈50 h and subsequently oxidized only slowly in air. These surfaces also displayed long charge carrier lifetimes and low surface recombination velocities, demonstrating that they are well-passivated electrically even during native oxide growth. Similar behavior was observed for surfaces that were functionalized using Cl_2(g) as the chlorinating agent. Methylation using the chlorination/alkylation routes produced the lowest surface recombination velocities of all the alkyl groups studied, although good chemical stability and a high degree of electrical passivation was also observed for the other alkyl overlayers on the Si(111) surface. In contrast, surfaces functionalized by the Lewis acid-mediated reduction of a terminal alkene directly on the H-terminated Si(111) oxidized rapidly in air and exhibited higher surface recombination velocities. Methyl-terminated Si(111) surfaces prepared by electrochemical anodization of the Si in CH_3MgI−diethyl ether solutions displayed extensive oxidation in air and exhibited significantly higher surface recombination velocities than the other alkylated surfaces.

Acknowledgment. We acknowledge the National Science Foundation, Grant CHE-0213589, for support of this work and for providing a graduate research fellowship to L.J.W.

References and Notes

(1) Royea, W. J.; Juang, A.; Lewis, N. S. *Appl. Phys. Lett.* **2000**, *77*, 1988−1990.
(2) Bent, S. F. *Surf. Sci.* **2002**, *500*, 879−903.
(3) Mitchell, S. A.; Boukherroub, R.; Anderson, S. *J. Phys. Chem. B* **2000**, *104*, 7668−7676.
(4) Yu, H. Z.; Boukherroub, R.; Morin, S.; Wayner, D. D. M. *Electrochem. Commun.* **2000**, *2*, 562−566.
(5) Bansal, A.; Li, X.; Yi, S. I.; Weinberg, W. H.; Lewis, N. S. *J. Phys. Chem. B* **2001**, *105*, 10266−10277.
(6) Bansal, A.; Li, X. L.; Lauermann, I.; Lewis, N. S.; Yi, S. I.; Weinberg, W. H. *J. Am. Chem. Soc.* **1996**, *118*, 7225−7226.
(7) He, J.; Patitsas, S. N.; Preston, K. F.; Wolkow, R. A.; Wayner, D. D. M. *Chem. Phys. Lett.* **1998**, *286*, 508−514.
(8) Okubo, T.; Tsuchiya, H.; Sadakata, M.; Yasuda, T.; Tanaka, K. *Appl. Surf. Sci.* **2001**, *171*, 252−256.
(9) Terry, J.; Linford, M. R.; Wigren, C.; Cao, R. Y.; Pianetta, P.; Chidsey, C. E. D. *Appl. Phys. Lett.* **1997**, *71*, 1056−1058.
(10) Terry, J.; Linford, M. R.; Wigren, C.; Cao, R. Y.; Pianetta, P.; Chidsey, C. E. D. *J. Appl. Phys.* **1999**, *85*, 213−221.
(11) Boukherroub, R.; Wayner, D. D. M. *J. Am. Chem. Soc.* **1999**, *121*, 11513−11515.
(12) Cicero, R. L.; Linford, M. R.; Chidsey, C. E. D. *Langmuir* **2000**, *16*, 5688−5695.
(13) Effenberger, F.; Gotz, G.; Bidlingmaier, B.; Wezstein, M. *Angew. Chem., Int. Ed.* **1998**, *37*, 2462−2464.
(14) Terry, J.; Mo, R.; Wigren, C.; Cao, R. Y.; Mount, G.; Pianetta, P.; Linford, M. R.; Chidsey, C. E. D. *Nucl. Instrum. Methods Phys. Res., Sect. B* **1997**, *133*, 94−101.
(15) Linford, M. R.; Chidsey, C. E. D. *J. Am. Chem. Soc.* **1993**, *115*, 12631−12632.
(16) Linford, M. R.; Fenter, P.; Eisenberger, P. M.; Chidsey, C. E. D. *J. Am. Chem. Soc.* **1995**, *117*, 3145−3155.
(17) Sieval, A. B.; Demirel, A. L.; Nissink, J. W. M.; Linford, M. R.; van der Maas, J. H.; de Jeu, W. H.; Zuilhof, H.; Sudholter, E. J. R. *Langmuir* **1998**, *14*, 1759−1768.
(18) Sieval, A. B.; Linke, R.; Heij, G.; Meijer, G.; Zuilhof, H.; Sudholter, E. J. R. *Langmuir* **2001**, *17*, 7554−7559.
(19) Sung, M. M.; Kluth, G. J.; Yauw, O. W.; Maboudian, R. *Langmuir* **1997**, *13*, 6164−6168.
(20) Boukherroub, R.; Wojtyk, J. T. C.; Wayner, D. D. M.; Lockwood, D. J. *J. Electrochem. Soc.* **2002**, *149*, H59−H63.
(21) Boukherroub, R.; Wayner, D. D. M.; Lockwood, D. J.; Canham, L. T. *J. Electrochem. Soc.* **2001**, *148*, H91−H97.
(22) Boukherroub, R.; Wayner, D. D. M.; Sproule, G. I.; Lockwood, D. J.; Canham, L. T. *Nano Lett.* **2001**, *1*, 713−717.
(23) Boukherroub, R.; Morin, S.; Bensebaa, F.; Wayner, D. D. M. *Langmuir* **1999**, *15*, 3831−3835.
(24) Buriak, J. M.; Allen, M. J. *J. Am. Chem. Soc.* **1998**, *120*, 1339−1340.
(25) Buriak, J. M.; Stewart, M. P.; Geders, T. W.; Allen, M. J.; Choi, H. C.; Smith, J.; Raftery, D.; Canham, L. T. *J. Am. Chem. Soc.* **1999**, *121*, 11491−11502.
(26) Zazzera, L. A.; Evans, J. F.; Deruelle, M.; Tirrell, M.; Kessel, C. R.; McKeown, P. *J. Electrochem. Soc.* **1997**, *144*, 2184−2189.
(27) Schmeltzer, J. M.; Porter, L. A.; Stewart, M. P.; Buriak, J. M. *Langmuir* **2002**, *18*, 2971−2974.
(28) Cicero, R. L.; Chidsey, C. E. D.; Lopinski, G. P.; Wayner, D. D. M.; Wolkow, R. A. *Langmuir* **2002**, *18*, 305−307.
(29) Saghatelian, A.; Buriak, J. M.; Lin, V. S. Y.; Ghadiri, M. R. *Tetrahedron* **2001**, *57*, 5131−5136.
(30) Allongue, P.; de Villeneuve, C. H.; Pinson, J. *Electrochim. Acta* **2000**, *45*, 3241−3248.
(31) Allongue, P.; de Villeneuve, C. H.; Pinson, J.; Ozanam, F.; Chazalviel, J. N.; Wallart, X. *Electrochim. Acta* **1998**, *43*, 2791−2798.
(32) Dubois, T.; Ozanam, F.; Chazalviel, J.-N. *Electrochem. Soc. Proc.* **1997**, *97-7*, 296−310.
(33) Fidélis, A.; Ozanam, F.; Chazalviel, J. N. *Surf. Sci.* **2000**, *444*, L7−L10.
(34) Gros-Jean, M.; Herino, R.; Chazalviel, J. N.; Ozanam, F.; Lincot, D. *Mater. Sci. Eng. B* **2000**, *69*, 77−80.
(35) Henry de Villeneuve, C.; Pinson, J.; Bernard, M. C.; Allongue, P. *J. Phys. Chem. B* **1997**, *101*, 2415−2420.
(36) Haber, J. A.; Lewis, N. S. *J. Phys. Chem. B* **2002**, *106*, 3639−3656.
(37) Himpsel, F. J.; McFeeley, F. R.; Taleb-Ibrahimi, A.; Yarmoff, J. A.; Hollinger, G. *Phys. Rev. B* **1988**, *38*, 6084−6096.
(38) Seah, M. P. In *Practical Surface Analysis*, 2nd ed.; Briggs, D., Seah, M. P., Eds.; Wiley: Chichester, U.K., 1990; Vol. 1, pp 201−255.
(39) Sturzenegger, M.; Prokopuk, N.; Kenyon, C. N.; Royea, W. J.; Lewis, N. S. *J. Phys. Chem. B* **1999**, *103*, 10838−10849.
(40) Sze, S. M. *The Physics of Semiconductor Devices*, 2nd ed.; Wiley: New York, 1981.
(41) Yablonovitch, E.; Gmitter, T. J. *Solid-State Electron.* **1992**, *35*, 261−267.
(42) Asao, N.; Sudo, T.; Yamamoto, Y. *J. Org. Chem.* **1996**, *61*, 7654−7655.
(43) Sudo, T.; Asao, N.; Gevorgyan, V.; Yamamoto, Y. *J. Org. Chem.* **1999**, *64*, 2494−2499.